Highly efficient single-pass second harmonic generation in a periodically poled $MgO:LiNbO_3$ waveguide pumped by a fiber laser at 1111.6 nm

Hailing Jiang, Guohui Li,and Xinye Xu*

State Key Laboratory of Precision Spectroscopy, Department of Physics, East China Normal University, Shanghai, 200062, China

** xyxu@phy.ecnu.edu.cn*

Abstract: A green light at 556 nm is generated by direct frequency doubling of a fiber laser at 1111.6 nm with a periodically poled MgO:LiNbO3 waveguide. We have investigated optical inhomogeneities by measuring the temperature tuning curve of second harmonic generation, and the obtained parameters are used for identifying the uniformity of the waveguide. The thermal dephasing could be diminished by adjusting the crystal temperature, and the conversion efficiency was maximized. Finally, an output power of 111.8 mW at 556 nm was generated with 213 mW of coupled fundamental light under optimum conditions, which corresponds to 52.5% conversion efficiency.

OCIS codes: (060.4370) Nonlinear optics, fibers; (140.3515) Lasers, frequency doubled; (190.2620) Harmonic generation and mixing; (130.7405) Wavelength conversion devices.

References and links

1. A. D. Ludlow, T. Zelevinsky, G. K. Campbell, S. Blatt, M. M. Boyd, M. H. G. de Miranda, M. J. Martin, J. W. Thomsen, S. M. Foreman, J. Ye, T. M. Fortier, J. E. Stalnaker, S. A. Diddams, Y. Le Coq, Z. W. Barber, N. Poli, N. D. Lemke, K. M. Beck, and C. W. Oates, "Sr lattice clock at 1 x $10(-^{16})$ fractional uncertainty by remote optical evaluation with a Ca clock," Science **319**(5871), 1805–1808 (2008).
2. T. Vo-Dinh, B. Cullum, and P. Kasili, "Development of a multi-spectral imaging system for medical applications," J. Phys. D Appl. Phys. **36**(14), 1663–1668 (2003).
3. N. Poli, Z. W. Barber, N. D. Lemke, C. W. Oates, L. S. Ma, J. E. Stalnaker, T. M. Fortier, S. A. Diddams, L. Hollberg, J. C. Bergquist, A. Brusch, S. Jefferts, T. Heavner, and T. Parker, "Frequency evaluation of the doubly forbidden $^1S_0$-$^3P_0$ transition in bosonic ^{174}Yb," Phys. Rev. A **77**(5), 050501 (2008).
4. T. Kuwamoto, K. Honda, Y. Takahashi, and T. Yabuzaki, "Magneto-optical trapping of Yb atoms using an intercombination transition," Phys. Rev. A **60**(2), R745–R748 (1999).
5. R. Maruyama, R. H. Wynar, M. V. Romalis, A. Andalkar, M. D. Swallows, C. E. Pearson, and E. N. Fortson, "Investigation of sub-Doppler cooling in an ytterbium magneto-optical trap," Phys. Rev. A **68**(1), 011403 (2003).
6. F. Villa, A. Chiummo, E. Giacobino, and A. Bramati, "High-efficiency blue-light generation with a ring cavity with periodically poled KTP," J. Opt. Soc. Am. B **24**(3), 576–580 (2007).
7. F. Torabi-Goudarzi, and E. Riis, "Efficient cw high-power frequency doubling in periodically poled KTP," Opt. Commun. **227**(4-6), 389–403 (2003).
8. A. Bouchier, G. Lucas-Leclin, P. Georges, and J. M. Maillard, "Frequency doubling of an efficient continuous wave single-mode Yb-doped fiber laser at 978 nm in a periodically-poled $MgO:LiNbO_3$ waveguide," Opt. Express **13**(18), 6974–6979 (2005).
9. K. Sakai, Y. Koyata, and Y. Hirano, "Blue light generation in a ridge waveguide $MgO:LiNbO_3$ crystal pumped by a fiber Bragg grating stabilized laser diode," Opt. Lett. **32**(16), 2342–2344 (2007).
10. F. R. Nash, G. D. Boyd, M. Sargent III, and P. M. Bridenbaugh, "Effect of optical inhomogeneities on phase matching in nonlinear crystals," J. Appl. Phys. **41**(6), 2564–2576 (1970).
11. S. Helmfrid, and G. Arvidsson, "Influence of randomly varying domain lengths and nonuniform effective index on second-harmonic generation in quasi-phase-matching waveguides," J. Opt. Soc. Am. B **8**(4), 797–804 (1991).
12. S. Helmfrid, G. Arvidsson, and J. Webjörn, "Influence of various imperfections on the conversion efficiency of second-harmonic generation in quasi-phase-matching lithium niobate waveguides," J. Opt. Soc. Am. B **10**(2), 222–229 (1993).
13. C. W. Hoyt, Z. W. Barber, C. W. Oates, T. M. Fortier, S. A. Diddams, and L. Hollberg, "Observation and absolute frequency measurements of the $^1S_0$-$^3P_0$ optical clock transition in neutral ytterbium," Phys. Rev. Lett. **95**(8), 083003 (2005).

#114004 - $15.00 USD Received 8 Jul 2009; revised 19 Aug 2009; accepted 19 Aug 2009; published 26 Aug 2009

14. M. Yasuda, F.-L. Hong, T. Kurosu, T. Kohno, J. Ishikawa, A. Onae, O. Shin-ichi, and H. Katori, "Development of an optical lattice clock in NMIJ, AIST," in *Proceedings of the IEEE International Frequency Control Symposium and Exposition* (Miami, FL, 2006), pp. 284–286.
15. A. Yariv, "Coupled-mode theory for guided-wave optics," IEEE J. Quantum Electron. **QE-9**(9), 919–933 (1973).
16. K. R. Parameswaran, J. R. Kurz, R. V. Roussev, and M. M. Fejer, "Observation of 99% pump depletion in single-pass second-harmonic generation in a periodically poled lithium niobate waveguide," Opt. Lett. **27**(1), 43–45 (2002).
17. Z. M. Liao, S. A. Payne, J. Dawson, A. Drobshoff, C. Ebbers, D. Pennington, and L. Taylor, "Thermally induced dephasing in periodically poled KTP frequency-doubling crystals," J. Opt. Soc. Am. B **21**(12), 2191–2196 (2004).
18. M. M. Fejer, G. A. Magel, D. H. Jundt, and R. L. Byer, "Quasi-phase-matched second harmonic generation: tuning and tolerances," IEEE J. Quantum Electron. **28**(11), 2631–2654 (1992).
19. D. Eimerl, "Thermal aspec6ts of high-average-power electrooptic switches," IEEE J. Quantum Electron. **23**(12), 2238–2251 (1987).

1. Introduction

Stable and efficient continuous wave (cw) high-power laser sources in blue and green spectral regions are necessary for various applications such as optical atomic clocks, material processing, optical communication or medical diagnostics [1,2]. Currently, the ytterbium (Yb) atom has become one of the promising candidates for developing new generation optical frequency standards and metrology [3]. In order to construct Yb optical clocks, the two-stage Doppler cooling is needed, especially the $^1S_0$-$^3P_1$ transition at 556 nm is used for the second-stage cooling. In the early experiments, the dye lasers were widely applied for this second stage cooling [4,5]. However, except for generating the high output power, the dye lasers have some disadvantages, for instance, the system is large and complicated, the operation time of the dye is only a few days, and the maintenance cost is high. Therefore people are seeking some simple laser systems to replace this complex laser. One of such laser sources is produced by second harmonic generation (SHG), consisting of a pump laser and a frequency doubler [6–9]. For the 556 nm laser system, an Yb-doped fiber laser is preferred to be used as a pumping source because it has advantages over other types of lasers including: high output power, high optical quality, compact size, reliability and easy operation, especially its narrow line width.

The single-pass SHG by quasi-phase-matching (QPM) is an attractive way for achieving a frequency doubler for this particular application. It has the merits of simplicity and stability compared with the method of using a ring cavity which has been studied widely [6]. The highly efficient periodically poled materials, especially the periodically poled MgO:$LiNbO_3$ (PPMgLN), combined with the waveguide (WG) is an attractive way for achieving high conversion efficiency in the low power region. It has the following advantages: large nonlinear coefficient; higher resistance to the photorefractive damage with doped MgO; strong confinement of the fundamental light along the waveguide.

By frequency doubling of a single mode Yb-doped fiber laser at 978 nm, SHG power of 83 mW was generated with 26% conversion efficiency [8], and by using a fiber grating stabilized laser diode, SHG power of 73 mW with 27% conversion efficiency was achieved [9]. However, due to thermal dephasing, the experimental values were lower than the theoretical predicted values based on pump depletion in the high power region. The conversion efficiency was expected to be improved by decreasing light-absorbing defects using the purer quality crystal. The optical inhomogeneities were also found to limit the SHG conversion efficiency [10–12]. We have investigated this effect by measuring the SHG power as a function of the temperature of the waveguide.

In addition, a few groups have reported the experiments on making 556 nm light for cooling neutral Yb using an approach with the fiber laser and a frequency doubler. For instance, the power of 30 mW at 555.8 nm was generated by direct frequency doubling of a fiber laser using a 5 cm PPMgLN crystal in NIST [13]; a green laser with the power of 50 mW was obtained by direct frequency doubling of an Yb-doped fiber laser at 1111.6 nm using a periodically poled lithium niobate waveguide crystal in NMIJ, AIST [14]. However,

#114004 - $15.00 USD Received 8 Jul 2009; revised 19 Aug 2009; accepted 19 Aug 2009; published 26 Aug 2009

the SHG powers and conversion efficiencies reported previously all were lower than that described here.

In this paper, we present the experiments on generating the 556 nm laser source by direct frequency doubling of a fiber laser with a PPMgLN waveguide and investigating how to achieve a higher SHG conversion efficiency with the relative low pumping power. Our results show that the SHG power of 111.8 mW at 556 nm with 52.5% single-pass conversion efficiency has been achieved by direct frequency doubling of a fiber laser with a PPMgLN waveguide.

2. Experimental setup

The experimental setup used for SHG is shown schematically in Fig. 1. The fundamental light source was a cw single-mode Yb-doped fiber laser with the maximum output power of 700 mW at 1111.6 nm. The output light of the fiber laser was linearly polarized. The beam propagation parameter, M^2, of the fiber laser is below 1.1, and the linewidth of the fiber laser is < 50 kHz. The PPMgLN TEM_{00} WG device was fabricated by HC Photonics and has a pigtailed polarization maintaining fiber of 0.5 m. The PPMgLN crystal was designed for QPM SHG at 556 nm with a length of 20.01 mm, a width of 3.00 mm and a height of 0.5 mm. The light entrance and exit surfaces were anti-reflection coated for 1111.6 nm and 556 nm, respectively. The crystal was placed on a copper stage which was temperature-controlled by an oven within ± 0.1°C. To insure the uniformity of the PPMgLN temperature, a Teflon cover was put on top of the crystal.

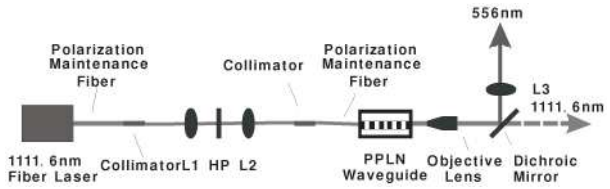

Fig. 1. Schematic of the experimental setup for direct frequency doubling of a fiber laser with a PPMgLN waveguide. It consists of a fiber laser, a PPLN waveguide, two collimators, three lenses (L1, L2, L3), a half-wave plate (HP), an objective lens and a dichroic mirror.

The output FC/APC connector of the fiber laser should not be directly connected with the input FC/APC connector of the WG, which was required by the manufacturer for safety issues. Therefore, we introduced a free-space coupling method to align the fundamental light to the WG device. As shown in Fig. 1, the coupling system was formed by two fiber collimators and two beam-shaping lenses with the same focal length of 7.5 cm. Since the polarization direction of the fundamental light might be not parallel with one of the birefringence axes of the fiber of the WG, a half-wave plate in front of the collimator connected to the pigtailed fiber was used to rotate the polarization direction of the fundamental light to maximize the coupling efficiency.

The highly divergent SHG light was first focused by an objective lens with the focal length of 10 mm. Then a dichroic mirror was used to separate the SHG light from the intense fundamental light. Finally, the green light was collimated by a lens with the focal length of 7.5 cm.

3. Optimization of SHG

In order to find the optimum QPM temperature, we scanned the crystal temperature with a fundamental light power of 119 mW (measured after the lens L2). The dependence of SHG power on the PPMgLN temperature was illustrated in Fig. 2. We found that the maximum output SHG power was 22.35 mW at the temperature of 55°C. To improve the measurement precision, for each data in this paper we did four measurements, which means that in all figures each data point represents the average of four measurements, and the error bars represent standard errors.

#114004 - $15.00 USD Received 8 Jul 2009; revised 19 Aug 2009; accepted 19 Aug 2009; published 26 Aug 2009

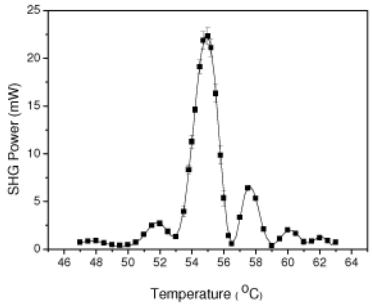

Fig. 2. SHG power as a function of the PPMgLN temperature, taken with the fundamental power of 119 mW. Dots are the experimental data. The solid line is the fitting curve.

As shown in Fig. 2, the observed multiple-peak temperature dependences is deviated from the sinc^2 functions predicted by the coupled-mode theory [15], which might be caused by the optical inhomogeneities, especially the non-uniformity of the refractive index along the pull axis in the growth process [10]. We regard different parts of the WG are phase matched at different temperatures. Assuming that the waveguide is composed of N regions with different length l_i, single-pass nonlinear conversion efficiency $\eta_{i,j}$, and different QPM temperatures, the SHG power can be written as

$$P_{2w} = \sum_{i=1}^{N} \eta_i P_w^2 \frac{\sin^2(\Delta k_i l_i / 2)}{(l_i \Delta k_i / 2)^2} + 2\sum_{i=1}^{N-1} \sum_{j=i+1}^{N} \sqrt{\eta_i \eta_j} P_w^2 \frac{\sin(\Delta k_i l_i / 2)}{(\Delta k_i l_i / 2)} \frac{\sin(\Delta k_j l_j / 2)}{(\Delta k_j l_j / 2)} \cos[\frac{(\Delta k_i l_i / 2)}{2} - \frac{(\Delta k_j l_j / 2)}{2}], \quad (1)$$

where P_{2w} (P_w) is the SHG (fundamental) power, $\Delta k_{i,j}$ is the phase mismatch in QPM corresponding to different inhomogeneous regions and is given by

$$\Delta k = \Delta k' - k_m, \quad (2)$$

where $\Delta k' = \frac{4\pi}{\lambda}(n_{2w} - n_w)$ is the normal phase mismatch, n_{2w} (n_w) is temperature-dependent indices for the SHG (fundamental) light, λ is the wavelength of the fundamental light and k_m is the mth-harmonic grating wave vector. Assuming that the phase mismatch should be approximately a linear function of the temperature, the phase mismatch Δk as a function of the crystal temperature T can be expanded in a Taylor series expansion at the phase-matching temperature T_p

$$\Delta k = \frac{4\pi}{\lambda} \frac{\partial \Delta n}{\partial T} (T - T_p), \quad (3)$$

where $\Delta n = n_{2w} - n_w$. The experimental data were fitted very well by the fitting formula (1) with N= 7, as shown in Fig. 2. We found that due to the optical inhomogeneities the SHG conversion efficiency was decreased by shortening the effective phase-matching length.

#114004 - $15.00 USD Received 8 Jul 2009; revised 19 Aug 2009; accepted 19 Aug 2009; published 26 Aug 2009

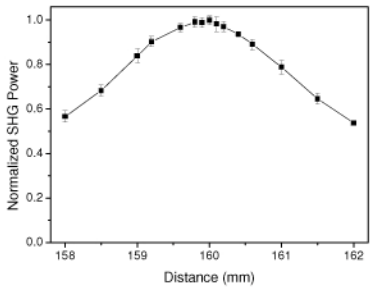

Fig. 3. Normalized SHG power at 556 nm versus the distance between two beam-shaping lenses, when the fundamental power is 51.5 mW and the crystal temperature is 55°C.

The microscope objective lens combined with a precision translation stage is usually adopted to improve the fiber coupling efficiency. However, the coupling efficiency with the microscope objective lens method is relative low and unstable in a single-mode fiber coupling. In this experiment, as shown in Fig. 1, two fiber collimators with the same focal length of 11.0 mm and the numerical aperture NA=0.25 were used. Two beam-shaping lenses (L1, L2) were used to control the beam size in the transverse direction and the beam divergence angle along the propagation direction of the fundamental light, and the latter was more important than the former. L2 was placed on a two-dimensional linear stage. The SHG power (normalized) as a function of the distance between the two beam-shaping lenses was shown in Fig. 3. By using the free-space coupling method, 69% coupling efficiency was achieved.

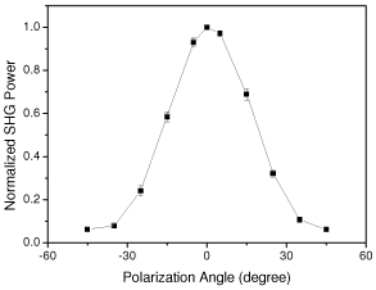

Fig. 4. Normalized SHG power at 556 nm versus polarization angle, taken with approximately 51.5 mW fundamental input power and the crystal temperature at 55°C.

In addition, by rotating the half-wave plate to change the polarization direction of the incident fundamental light, the SHG power (normalized) was maximized as shown in Fig. 4, here the angle was defined as the intersecting angle between polarization direction of the fundamental light and one of birefringence axes of the pigtailed fiber.

#114004 - $15.00 USD Received 8 Jul 2009; revised 19 Aug 2009; accepted 19 Aug 2009; published 26 Aug 2009

4. Experimental results and analysis

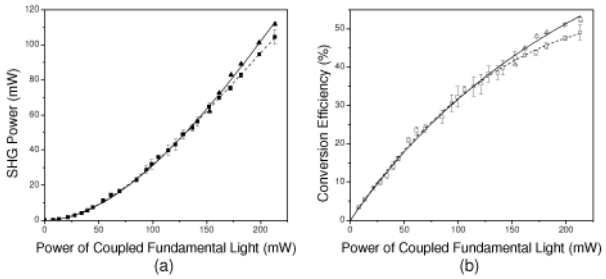

Fig. 5. (a) SHG power as a function of the fundamental power coupled into the waveguide. Solid squares: experimental data measured by setting the crystal temperature at 55°C; solid triangles: the experimental data measured with the temperature adjusted to yield maximum second harmonic power; solid line: the $\tanh^2$ fits; dashed line: theoretical fits when thermal dephasing and pump depletion are taken into account. (b) SHG conversion efficiency versus coupled fundamental power; open squares: conversion efficiency with the crystal temperature of 55°C; open triangles: the experimental data measured with the temperature adjusted to yield the maximum conversion efficiency; solid line: the $\tanh^2$ fits; dashed line: theoretical fits when thermal dephasing and pump depletion are taken into account.

Figure 5(a) shows the SHG power (P_{SHG}) as a function of the fundamental power ($P_{coupled}$) coupled into the WG under the optimum conditions. Figure 5(b) shows the SHG conversion efficiency as a function of the coupled fundamental light power. Under the strong pump depletion approximation, the dependence of SHG power on the coupled fundamental power can be given by [16]

$$P_{SHG} = P_{coupled} \tanh^2(\sqrt{\eta P_{coupled}}), \tag{4}$$

where η is the single-pass nonlinear conversion efficiency. The experimental data (solid squares) were well fitted by Eq. (4) for a coupled fundamental light power less than 162 mW. The single-pass nonlinear conversion efficiency is evaluated to be about 401% /W. However, with an increased fundamental power we have found a deviation between the experimental data (solid squares) and the theoretical calculation (solid line) as shown in Fig. 5. This deviation may be caused by the thermal dephasing [17]. Following the Ref [18], when the thermal dephasing and the pump depletion are considered, the SHG power could be approximately written as

$$P_{SHG} = gP_{coupled} \tanh^2(\sqrt{\eta P_{coupled}}), \tag{5}$$

where $g(\Delta T) = \sin c^2[\frac{\Delta kL}{2}(\Delta T + \delta T)]$ is the thermal dephasing factor, Δk is the phase mismatch, L is the crystal length, δT is an alignment factor [17] that accounts for the initial non-optimal QPM temperature and ΔT is the temperature difference which can be calculated by solving Poisson's equation [19]. The experimental data were fitted very well by Eq. (5), shown as the dashed line in Fig. 5, which indicated the thermal dephasing was a dominant effect for the coupled fundamental power higher than 162 mW. We then carefully tuned the PPMgLN temperature to compensate the phase mismatch caused by the thermal dephasing for the coupled fundamental power higher than 153 mW to optimize the conversion efficiency. For the coupled power of 153 mW, the oven temperature was 55°C; for the coupled power of 162 mW and 173 mW, it was 54.7°C; for the coupled power of 182 mW, 199 mW and 213 mW, it was 54.6°C. The optimum phase-matching temperature was 0-0.4°C lower than 55°C

#114004 - $15.00 USD Received 8 Jul 2009; revised 19 Aug 2009; accepted 19 Aug 2009; published 26 Aug 2009

with $P_{coupled}$ from 153 mW to 213 mW. The optimized SHG power (solid triangles) and conversion efficiency (open triangles) agree well with the theoretical predictions based on Eq. (4) shown as the solid lines. In this experiment the defect absorption was not observed, therefore, by lowering the oven temperature, the SHG power could be recovered. Finally the maximum SHG power of 111.8 mW has been obtained with 213 mW of the coupled fundamental power, which corresponds to 52.5% conversion efficiency.

We like to note that there are a few weaknesses of this technique. For instance, the degradation of the SHG efficiency over a short time would be expected, and even it would be worse at high power region. Fortunately, so far we haven't seen this phenomenon in our apparatus due to the following reasons. One is that we have been running this laser system only for a few months, and the SHG output power needed for daily operation was about 40 mW, occasionally being 80 mW and even more; the other is that our waveguide was annealed, which maybe help suppress this effect. Another shortcoming is that the input fundamental light power for the waveguide is restricted for having a longer lifetime of the device, so that the SHG output power would be limited. In our case, the maximum coupled fundamental power was suggested to be around 220 mW.

As shown in Fig. 6, the frequency tuning range of the SHG light was measured to be about 15.6 GHz, which was limited by the PZT tuning range of the 1111.6 nm fiber laser. We found that the maximum change of the output SHG light power was less than 5% within 15.6 GHz frequency scanning range. It would be good for applications involving atom manipulation.

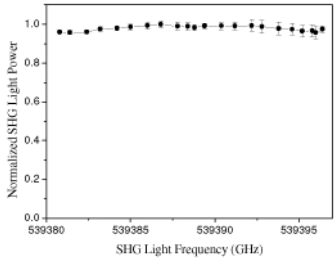

Fig. 6. The normalized SHG light power versus the frequency of the SHG light. Frequency tuning range of the SHG light was determined to be about 15.6 GHz.

The beam quality of the SHG light was measured. Figure 7 shows the transverse pattern of the green light, and its beam shape was slightly elliptical. A hyperbolic fit was performed to obtain the beam propagation factor M^2~1.1 (1.05±0.01 in the horizontal direction and 1.17±0.01 in the vertical direction in Fig. 7).

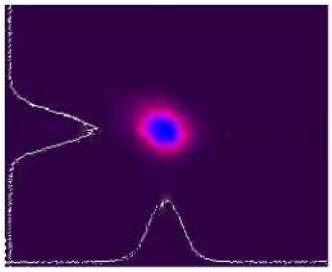

Fig. 7. The transverse pattern of the green light. The beam propagation factor M^2 was determined to be about 1.1.

5. Conclusions

We have investigated the influences of the temperature, distance between two beam-shaping lenses and polarization of the fundamental light upon the QPM SHG, and the optimum

#114004 - $15.00 USD Received 8 Jul 2009; revised 19 Aug 2009; accepted 19 Aug 2009; published 26 Aug 2009

operating conditions for the frequency doubling have been obtained. A maximum output power of 111.8 mW at 556 nm with 52.5% conversion efficiency has been achieved. To our knowledge, it represents the highest values ever obtained with 1111.6 nm fiber lasers in a single-pass configuration. Inhomogeneities and thermal dephasing were found to reduce the conversion efficiency. The former can be minimized if the more uniform crystal is obtained by carefully controlling the crystal growth process, and in our experiment the latter could be diminished by adjusting the oven temperature. The green light at 556 nm could be used for cooling and trapping of Yb atoms, quantum manipulation, quantum computation and optical atomic clock. Next step, by using this laser system we will realize the second-stage cooling on the $^1S_0$-$^3P_1$ intercombination transition at 556 nm of Yb atoms.

Acknowledgements

This work is supported by the National Natural Science Foundation of China under grant 10774044, the National Key Basic Research and Development Program of China under grant 2006CB921104, the Science and Technology Commission of Shanghai Municipality of China under grant 07JC14019, Shanghai Pujiang Talent Program of China under grant 07PJ14038, and the Ph.D. Program Scholarship Fund of ECNU 2009.

#114004 - $15.00 USD Received 8 Jul 2009; revised 19 Aug 2009; accepted 19 Aug 2009; published 26 Aug 2009